Postprint of: Abdoli H., Molin S., Farnoush H., Effect of interconnect coating procedure on solid oxide fuel cell performance, Materials Letters, Vol. 259 (2020), 126898, DOI: 10.1016/j.matlet.2019.126898

Effect of interconnect coating procedure on solid oxide fuel cell performance

Hamid Abdoli[1,*], Sebastian Molin[2], Hamidreza Farnoush[3]

[1] Department of Renewable Energy, Niroo Research Institute, P.O. Box: 1468613113, Tehran, Iran.

[2] Faculty of Electronics, Telecommunications and Informatics, Gdańsk University of Technology, ul. G. Narutowicza 11/12, 80-233 Gdańsk, Poland.

[3] Department of Metallurgy and Materials Engineering, Faculty of Engineering, University of Kashan, P.O. Box: 87317-51167, Kashan, Iran.

Abstract

Chromium (Cr) species vaporizing from chromia-forming alloy interconnects is known as a source of degradation in solid oxide fuel cell (SOFC) stacks called "cathode poisoning". $(Mn,Co)_3O_4$ spinel coatings offer good protection against Cr evaporation during operation. In this study, Crofer 22 APU steel interconnects were electrophoretically deposited in different mediums to obtain high packing of green coating layer. The optimized sample was then sintered in air-atmosphere or dual-atmospheres (reducing-oxidizing). Anode-supported cells were exposed from cathode side to bare or coated interconnects for 100 h at 800 °C. The electrochemical performances of aged cells were compared at 800 ˚C. Due to higher density coating obtained by dual-atmospheres sintering process, the exposed cell showed performance similar to non-poisoned cell (0.95-0.98 W/cm^2). The cell exposed to air-atmosphere sintered coating interconnect showed lower output power (0.75 W/cm^2) due to coating lower density. The cell exposed to uncoated interconnect exhibited considerable degradation and the lowest power (0.66 W/cm^2).

Keywords: Sintering; Colloidal processing; Electrophoretic deposition; SOFC; Interconnect; Electroceramics

* Correspong author: hamidabdoli@yahoo.com

1. Introduction

Generally SOFC stacks experience a gradual reduction in performance and efficiency induced by degradation of internal elements. Under working conditions of SOFC, the ferritic stainless steels used as interconnects are oxidized, forming a Cr_2O_3 and $(Mn,Cr)_3O_4$ scale on the surface which decreases electrical conductivity of stack and output power [1]. Moreover, the oxide scales prone to form volatile Cr(VI)-species that degrade the SOFC cathode performance which is *so-called* as "cathode poisoning". The oxygen potential difference induced by the electrochemical oxygen reduction at gas/cathode/electrolyte triple-phase-boundary (TPB) interfaces, and/or the chemical affinity of the cathode materials with Cr vapors on the surface are considered as the driving forces of the Cr reaction at the cathode [2]. These two phenomena can cause an irreversible and severe degradation of the fuel cell stack.

A way to mitigate these adverse effects is to coat the FSS inerconnect with a protective, electrically conductive material. $(Mn,Co)_3O_4$ spinels (MCO) are promising materials for the air side of the interconnect [3]. Various techniques have been used to apply a dense, adherent and stable coating on interconnects. Electrophoretic deposition (EPD) is a versatile method because of its low-cost, simplicity and flexibility [4]. The effective parameters on EPD coating density were studided in our pervious report [5]. Dense coating successfully blocks the evaporation of volatile Cr-species, increase the effective electrical conductivity and stop crack propagation. The effect of sintering conditions of slurry coated interconnects on its density, microstructure and oxidation resistance behavior is studied previously [3,7]. Effective sintering of MCO spinel coatings on the basis of dual atmosphere sintering has been proposed by Yang et al. [7]. Some studies has been published on the effect of additives [8], temperature and gas compositions [3] on the resultant coating microstructure. However, the influence of resultant coating on cell performance and/or degradation has not been reported which is the aim of the current report.

2. Materials and Methods

One-inch diameter ceramic button cells were fabricated of NiO/8YSZ anode-support layer (ASL~400µm), a NiO/8YSZ anode-functional layer (AFL~50µm), an 8YSZ electrolyte layer (EL~10µm), and a LSM cathode layer (CL~50µm). Half-cells were made by tape-casting of anode and electrolyte layers, followed by sintering at 1400˚C for 10 h. A CL with 1 cm^2 effective area was applied by screen-printing and sintered at 1200˚C for 2 h.

Crofer 22APU alloy plates with the dimensions of 20 mm ×20 mm ×0.3 mm were used as the source of Cr-species. EPD procedure was conducted under constant voltage of 20 V for 30-240 s [5]. The optimized sample was sintered in: 1) air for 2 h at 900 ˚C, and 2) dual atmosphere for 5 h in H_2 at 850 ˚C and oxidizing for 24 h in air. The microstructures of coatings were examined by scanning electron microscopy (Hitachi, Japan).

Cells were inserted in an alumina jig, connecting the contact materials (Pt mesh, paste and wires). A interconnect part was put close to the cathode side and the assembly was sealed using ceramic cement. Samples were thermally-aged for 100 h at 800 °C naming: 1) B-Cell: exposed to bare interconnect, 2) A-Cell: exposed to air-sintered coated interconnect, and 3) DA-Cell: exposed to dual-atmosphere-sintered coated interconnect. An as-prepared reference cell was also used for comparison (REF-Cell). Current-voltage characteristics and electrochemical impedance spectroscopy (EIS) of fabricated cells were measured once thermal aging was completed. For this aim, the anode was reduced at 850 ˚C for 10 h and then temperature was lowered to 800 ˚C. The humidified (3 vol% H_2O) hydrogen and air were used as fuel and oxidant, respectively, with a flow rate of 100 sccm.

3. Results and discussion

In order to obtain a high density EPD coating, kinetics behavior of particles packing was studied with deposition time. A general equation for densification mechanism of EPD coatings can be regarded [5]:

$$\frac{d\rho}{dt} = f(\rho)f(t) \tag{1}$$

where the densification rate ($\frac{d\rho}{dt}$) relates to the density ($f(\rho)$) and deposition time ($f(t)$) functions. A simple form of the equation is:

$$\frac{d\rho}{dt} = K'(1-\rho)t^{n-1} \tag{2}$$

where K' and n are constants. Integrating Eq. 2 with ρ=0 at t=0 leads to:

$$\ln\left(\frac{1}{1-\rho}\right) = Kt^n \tag{3}$$

The constant K gives a measure of the packing ability of the EPD. Fig. 1a shows the fitted density parameter ($\ln\left(\frac{1}{1-\rho}\right)$) in terms of deposition time by using Eq. 3 for the EPD of MCO particles from ethanol and isopropanol suspensions. The higher magnitude of packing ability for the deposition from isopropanol suspension (K_{isp}=0.0877) compared to ethanol suspension (K_{eth}=0.0397) indicates the higher coating quality achievement.

The SEM micrographs of the electrophoretically as-deposited MCO at 20 V for 180 s from ethanol and isopropanol suspensions are shown in Fig. 1b and c. EPD coatings were obtained from iodine dissolved suspensions as dispersant with concentration of 0.5 g.L^{-1} [5] which resulted in zeta potential of 47.4 ± 2.4 and 51.1 ± 1.5 mV for ethanol and isopropanol mediums, respectively. The deposited particles from isopropanol suspension have more close-packed microstructure while the one deposited from ethanol suspension includes agglomerated particles with less packing. The lower rate of deposition and viscosity in isopropanol suspension could cause particles to be arraanged in a close-packed structure. Also, the higher mobility and lower zeta potential of particles in ethanol suspension lead to the formation of large agglomerates in the microstructure, which is thought to be resulted from the high ionic strength of suspension and the low thickness of electrical double layer [9].

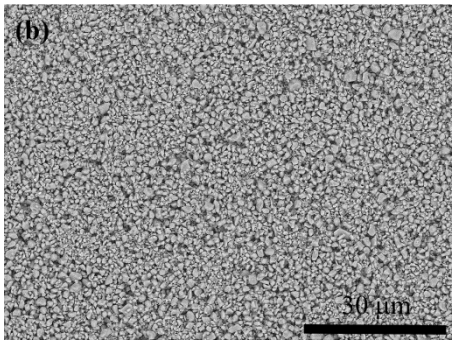

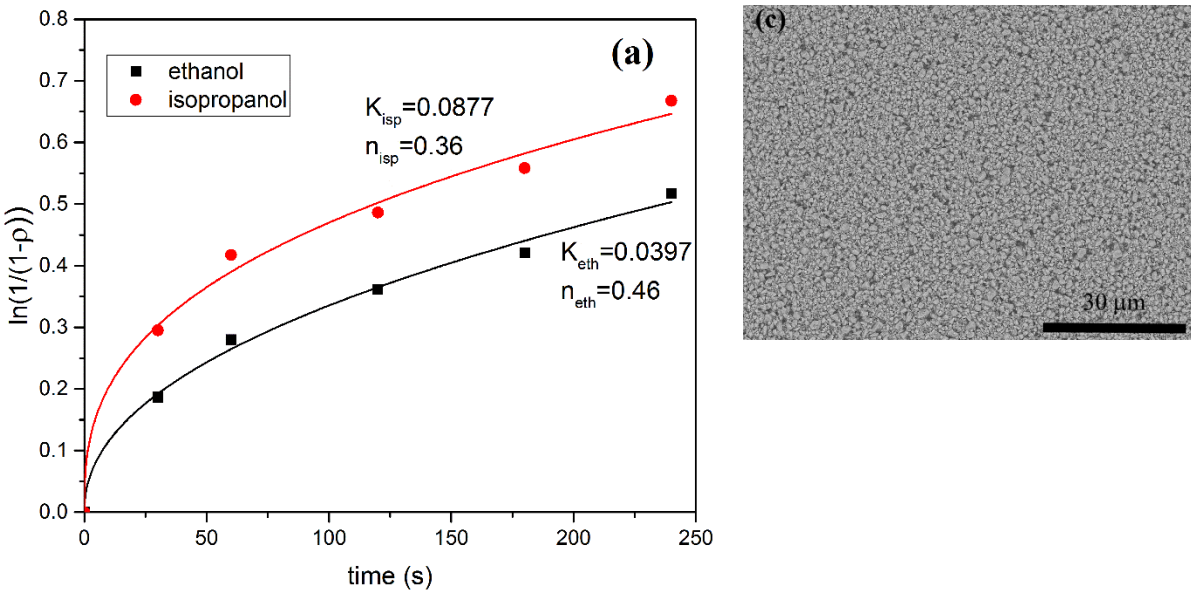

Fig. 1. (a) Densification curves against time fitted to Eq. 3; and related surface micrographs of EPD coating (20 V and 180 s) in (b) ethanol and (c) isopropanol.

The cross-sectional micrographs of the air sintered and dual-atmosphere sintered spinel coatings are depicted in Fig. 2a and b, respectively. While a thick oxide scale (composed of a Cr_2O_3 inner layer and a $(Mn,Cr)_3O_4$ spinel top layer) and porous microstructure was obtained after air-sintering process, a well-adhered and dense coating was resulted from dual-atmosphere sintering. This observation agrees with results previously reported by Lee et al. [10] and Smeacetto et al.[11]. Generally, heating above1100-1200 °C is required to densify MCO material in air [12]. Higher coating density could be achieved when the material is sintered under dual-atmosphere (reducing and oxidizing) at lower temperatures [2,13].

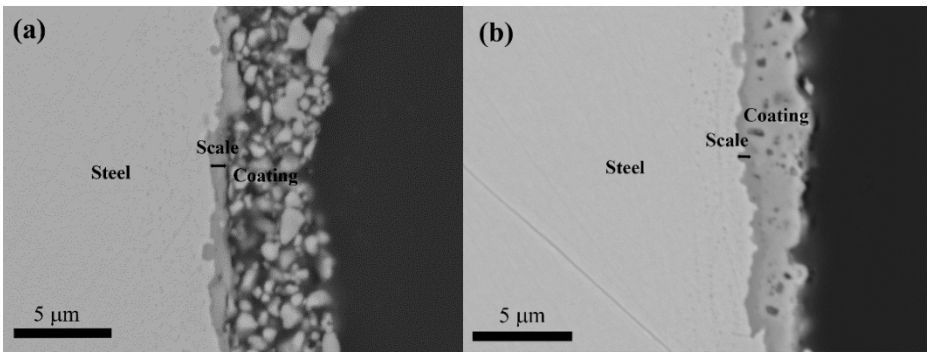

Fig. 2. Cross-sectional micrographs of MCO coatings; after (a) air-sintering (b) dual-atmosphere sintering.

In order to compare the effect of different coatings on chromium poisoning of SOFC cathodes, the electrochemical behavior of anode supported single cells was determined using EIS and I-V characterization. Fig. 3b shows the I-V and power density curves at 800 °C. It is seen that for DA-Cell the maximum power density (P_{max}) was similar to the REF-Cell, i.e. P_{max}≈0.95-0.98 W/cm^2. The minor difference are likely attributed to the reproducibility issues. However, in the presence of porous coatings, AS-Cell showed P_{max}≈0.75 W/cm^2. The lowest P_{max} was measured for the B-Cell, i.e. P_{max}≈0.66 W/cm^2.

Polarization resistances of the examined cells were measured by EIS and corresponded Nyquist plots at OCV are shown in Fig. 3b. The ohmic and polarization resistances (R_{ohm} and R_{pol}) of DA-Cell and REF-Cell were of close values. However, both R_{ohm} and R_{pol} were increased in the presence of porous coatings (32 % and 16 %, respectively). That could be due to formation of a thick chromia and Mn-Cr spinel which have lower conductivity than Mn-Co spinel. The electrical conductivity of the oxide scale is much lower in comparison to the metallic substrate and its growth results in monotonically increasing ASR values [4,14]. The highest R_{ohm} and R_{pol} was observed for B-Cell, where ~89 % and ~47 % increment was obtained in R_{ohm} and R_{pol} compared to REF-Cell, respectively, implying the effect of Cr evaporation on SOFC performance degradation.

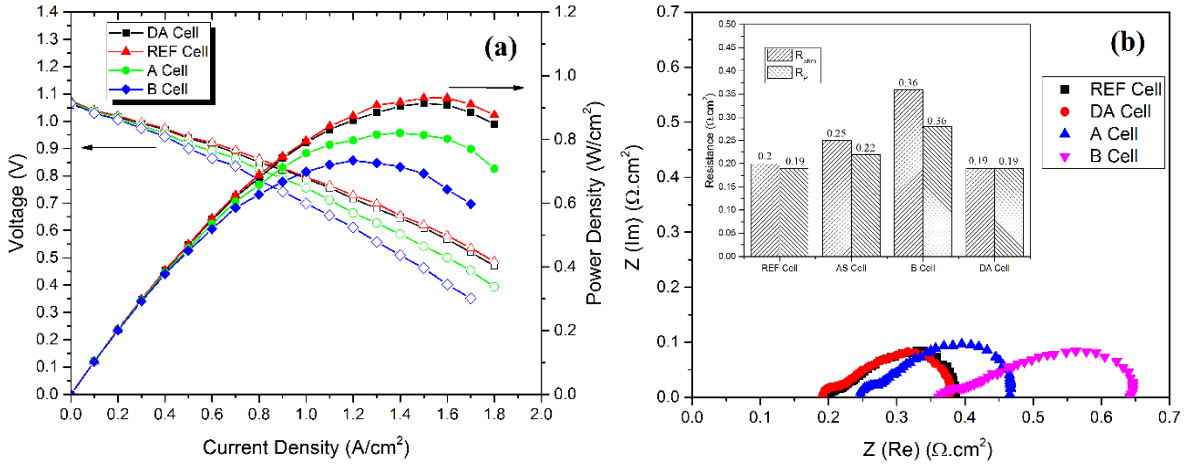

Fig. 3. (a) I-V and (b) Nyquist curves of the examined cells measured at 800 °C.

4. Conclusion

The effect of interconnect coating on electrochemical performance of anode-supported SOFCs were studied after exposing to steel interconnects with porous and dense as well as no coating. Coating procedure of $(Mn,Co)_3O_4$ powder was conducted via EPD and kinetics behavior of

particles packing was studied during the deposition process. Higher packing was obtained when ethanol suspension is replaced by isopropanol. Coatings were sintered under different atmospheres; i.e. at air for 2 h at 900 °C which led to a porous coating layer, and at dual atmosphere for 5 h in H_2 at 850 °C followed by oxidizing for 24 h in air which led to a dense and well-adhered coating. Coated interconnects were placed in the vicinity of ceramic cells for 100 h at 800 °C. The cell exposed to dense coating showed identical power density as well as ohmic and polarization resistances to those of the non-poisoned cell; i.e. no degradation was observed in cell performance. The cell exposed to the porous coating interconnect (i.e. lower quality coating) exhibited ~21% lower power density as well as ~32% and ~16% higher ohmic and polarization resistances, respectively. The ceramic cell exposed to the uncoated interconnect was also examined and degradation of ~32 % was observed in output power compared to the reference state.

References

[1] Y. Chou, J.W. Stevenson, J. Choi, J. Power Sources. 255 (2014) 1–8. doi:10.1016/j.jpowsour.2013.12.067.

[2] E. Zanchi, B. Talic, A.G. Sabato, S. Molin, A.R. Boccaccini, F. Smeacetto, J. Eur. Ceram. Soc. 39 (2019) 3768–3777. doi:10.1016/j.jeurceramsoc.2019.05.024.

[3] M. Bobruk, S. Molin, M. Chen, T. Brylewski, P. V Hendriksen, Mater. Lett. 213 (2018) 394–398. doi:10.1016/j.matlet.2017.12.046.

[4] S. Molin, A.G. Sabato, H. Javed, G. Cempura, A.R. Boccaccini, F. Smeacetto, Mater. Lett. 218 (2018) 329–333. doi:10.1016/j.matlet.2018.02.037.

[5] H. Abdoli, P. Alizadeh, Mater. Lett. 80 (2012) 53–55. doi:10.1016/j.matlet.2012.04.072.

[6] B. Talic, H. Falk-windisch, V. Venkatachalam, P. Vang, K. Wiik, H. Lea, J. Power Sources. 354 (2017) 57–67. doi:10.1016/j.jpowsour.2017.04.023.

[7] Z. Yang, G. Xia, Z. Nie, J. Templeton, J.W. Stevenson, Electrochem. Solid-State Lett. 8 (2008) B140–B143. doi:10.1149/1.2929066.

[8] C. J. Dileep Kumar, A. Dekich, H. Wang, Y. Liu, W. Tilson, J. Ganley, and J. W. Fergus, J. Electrochem. Soc. 161 (2014) F47-F53. doi: 10.1149/2.054401jes.

[9] H. Farnoush, Z. Rezaei, Ceram. Int. 43 (2017) 11885–11897. doi:10.1016/j.ceramint.2017.06.036.

[10] S. Lee, J. Hong, H. Kim, J. Son, J. Lee, B. Kim, H. Lee, K. Joong, 161 (2014) 1389–1394. doi:10.1149/2.0541414jes.

[11] F. Smeacetto, A. De Miranda, S. Cabanas, S. Molin, D. Boccaccini, M. Salvo, A.R. Boccaccini, J. Power Sources. 280 (2015) 379–386. doi:10.1016/j.jpowsour.2015.01.120.

[12] M. Mirzaei, A. Simchi, M.A. Faghihi-sani, A. Yazdanyar, Ceram. Int. 42 (2016) 6648–6656. doi:10.1016/j.ceramint.2016.01.012.

[13] A.G. Sabato, S. Molin, H. Javed, E. Zanchi, A.R. Boccaccini, F. Smeacetto, Ceram. Int. (2019) 0–1. doi:10.1016/j.ceramint.2019.06.161.

[14] H.R. Farnoush, H. Abdoli, S. Bozorgmehri, Procedia Mater. Sci. 11 (2015) 628–633. doi:10.1016/j.mspro.2015.11.099.

Figure Captions

Fig. 1. (a) Densification curves against time fitted to Eq. 3; and related surface micrographs of EPD coating (20 V and 180 s) in (b) ethanol and (c) isopropanol.

Fig. 2. Cross-sectional micrographs of MCO coatings; after (a) air-sintering (b) dual-atmosphere sintering.

Fig. 3. (a) I-V and (b) Nyquist curves of the examined cells measured at 800 °C.